J Mater Sci (2009) 44:1987–1997
DOI 10.1007/s10853-009-3293-2

Curing characteristics of an epoxy resin in the presence of ball-milled graphite particles

Soumen Jana · Wei-Hong (Katie) Zhong

Received: 13 October 2008 / Accepted: 22 January 2009 / Published online: 11 February 2009

Abstract The effects of simply-made graphite particles (GPs, 1 wt%) on curing kinetics of an epoxy resin were investigated by means of differential scanning calorimetry (DSC). Two approaches based on constant and variable activation energy were applied to analyze the DSC curves. Results from the constant energy method showed that addition of the GPs increased the activation energy E_c and the overall order of reaction $m + n$. With the variable energy method, the activation energy varied with curing conversion substantially in the GP/epoxy system; in contrast, the variation in the pure epoxy was very limited. The GPs also decreased the heat of reaction (ΔH) and increased the glass transition temperature (T_g) for the epoxy. Comprehensive analyses indicated that the GPs did not significantly impede the curing reaction, which can enable improvement of the composite functionalities without creating processing penalties. The information obtained from this study provides an understanding of multiple factors involved in the complex relationship of structure and properties of the composites.

Introduction

Epoxy resins are an important class of thermosetting polymers for various engineering applications due to their low density, good thermal, electrical and mechanical properties, potential self-healing properties, and have excellent processability for making structural components [1–3]. They can be cured with both anhydride and amide curing agents and in the curing process there is no release of small molecules [4]. However, further improvement of their properties is still desirable for some advanced applications, and incorporation of various nanosized additives into epoxy-based materials is one of the most notable approaches to solving this problem successfully [5, 6].

Additives with layered structure such as clay and graphite nanoplatelets are of interest due to their relatively low cost and their high specific surface area after exfoliation. Specifically, graphite derived at low cost and high production rate from graphite flakes can be used for creating multi-functional composites with high thermal and electrical conductivity [7, 8]. Wong and Yerramaddu found from their preliminary studies that carbon nanotubes and graphite nanoplatelets provide comparable mechanical properties (in-plane stiffness and strength) though their structures are different [7]. Therefore, additives made of graphite materials hold great promise as fundamental materials in making nanocomposites.

It is also important to consider the influence of graphitic additives on the curing kinetics of a pure epoxy as its properties depend on its crosslinked structure after curing. The morphology of epoxy network depends on the relative reaction rates of primary amine and secondary amine and is a vital parameter to achieve the information regarding network structure [8, 9]. Theoretically, in polymers, every point of the polymer chain that is available to participate in curing reactions does so. As the degree of reaction progresses toward completion, some points are locked into a position where there are no paired points for them to react with and, as a result, most polymers never actually reach a degree of cure of unity. Differential scanning calorimetry (DSC) exothermic curves can be used to study this extent of reaction and kinetic parameters of cure reaction with the

S. Jana · W.-H. Zhong (✉)
School of Mechanical and Materials Engineering,
Washington State University, Pullman, WA 99164, USA
e-mail: Katie_Zhong@wsu.edu

assumption that heat evolved is proportional to the extent of reaction [10–12].

Though it is commonly assumed that the curing reaction of thermoset polymers such as epoxy occurs as a single process, in fact it is very complex due to the occurrence of many simultaneous reactions, as well as due to changes in the curing phenomena, such as transitioning from chemical control to diffusion control, and the activation energy is believed to vary throughout the curing process. In addition, the presence of nanoparticles will most likely further add to the complexity. The method used to determine this variable activation energy depends on the extent of curing conversion without making any assumption on that conversion. In this paper we utilized both methods to find a comprehensive and more profound understanding of the curing kinetics of the epoxy systems.

Numerous studies on curing kinetics of thermoset in the presence of additives have been conducted. Buggy et al. [13] reported that addition of carbon fiber to epoxy resin hindered the curing process. Zhong et al. [14] observed similar phenomena with graphitic carbon nanofibers. Other nanoparticles such as silica, carbon black, carborandum, etc., also diminished the curing process as reported [15–18]. However, there are some reports in which no impact by fillers on curing kinetics of epoxy resins was found. For instance, Wang and Storm [19] did not find any significant difference in cure kinetics for both SPX 8800 epoxy prepreg and neat epoxy. Kaelble and coworkers [20] and Loustalot and Grenier [21] did not find substantial changes in curing mechanisms in their respective systems. From these reported studies, it can be observed that different additives showed different impacts on curing process, which ranged from negative to neutral depending on the additives and the base epoxy resins.

In our studies, a type of sub-micron "puffed" graphite particles (GPs) was developed from acid-treated graphite flakes by heating and ball milling, which are composed of disordered graphene sheets. Our previous investigation indicated that strength and toughness of the resulting epoxy composites were clearly increased to the extent of 23.0% (from 92.90 ± 17.20 to 114.33 ± 9.71 MPa) and 20.6% (from 1.26 ± 0.03 to 1.52 ± 0.07 MPa-$m^{1/2}$), respectively, through addition of the GPs into an epoxy resin (paper has been submitted to another journal). These results indicated the potential of the GPs as effective reinforcements for epoxy materials. The necessary next step is to study the curing kinetics of the GPs reinforced epoxy composites, in understanding the relationships between processing and performance. Although much effort has been made to understand the curing kinetics of epoxy resins with different kinds of fillers, the authors found no specific reports on the effects of the GPs on curing kinetics of thermoset resins. DSC and near-infrared spectroscopy (NIR) are several techniques to characterize the curing kinetics of thermoset polymers, Fourier transform infrared spectroscopy (FT-IR) and UV reflection spectroscopy (UVR) [22, 23]. Among them, DSC technologies have been most commonly applied. To find out the effects of the GPs on the curing reactions of an epoxy resin, experimental and theoretical analyses were made using both constant and variable activation energy methods.

Experimental

Materials

Expandable graphite flakes, obtained from Graftech International Ltd, were of specification 160–80 N, which means that their size as-received is 80 mesh, equal to 250 μm, and this particular type of graphite flakes start to expand at 160 °C. Though the as-received graphite flakes were acid-treated with a mixture of sulfuric and nitric acid (procedure can be found from website of Graftech International Ltd), they had neutral surface pH (reported by manufacturer) and were in expandable form. Epoxy resin, diglycidyl ether of bisphenol A (DGEBA) based epoxy resin, Epon® 828 and cure agents, Epikure™ W (diethyltoluenediamene [DETDA]), were purchased from Miller-Stephenson Chemical Inc.

Preparation of GPs

The as-received graphite flakes were placed in a clean cubicle and this cubicle was then positioned in an auto-controlled furnace at a temperature of 1,000 °C for 30 s for expansion through heating. The mechanism behind this exfoliation is mainly the generation and expansion of CO_2 in the interstices between the graphene sheets due to rapid heating. Moreover, this high-temperature heating might assist in removing impurities and intercalants present in expandable graphite flakes. Scanning electron microscope (SEM: JOEL Co.) was used to observe the expanded graphite flakes.

The expanded graphite flakes were then placed in a planetary ball mill (Fritsch Pulverisette 6 Planetary Mono Mill) to reduce the size of the scale particles. This mill had fifty 10 mm tungsten-carbide grinding balls. A total of 24-h milling was performed on the graphite flakes. However, the milling time was restricted due to heating and therefore each alternate 30 min was used for milling and then cooling due to heat generation (suggested by manufacturer). The average size (major length, since particles were not always spherical) of the particles measured using particle size analyzer was 400 nm, which is higher than the so-called nanoscale upper limit (<100 nm). However, we did not observe the size of 200 nm or less in the analyzer.

Fig. 1 TEM images of a graphite particle (scale: 100 nm)

Figure 1 shows the transmission electron microscopy (TEM) image of a typical graphite particle.

Preparation of composite specimens

The curing agent was added to the epoxy 828 in a ratio of 24:100 by weight. In total, 1 wt% GPs (w.r.t. pure epoxy) were mixed to the pure epoxy. A bath-sonifier was used for an hour at room temperature (25 °C) to disperse the GPs into the pure epoxy, followed by degassing of each kind of mixture conducted for 30 min to remove air bubbles. A homogeneous distribution of particles in the matrix was obtained.

Characterization techniques

X-ray diffraction

The inter-graphene d-spacing of particles was measured using a Philips PW1830 powder X-ray diffractometer instrument. X-ray diffraction (XRD) was carried out with Cu Kα radiation ($\lambda = 0.154$ nm) with a step wise of 0.05° and dwell time 1 s, working at 45 kV 40 mA.

Nanoindentation

Nanoindentation tests on as-received graphite flakes and prepared GPs were conducted. Each type was placed on glass substrates separately with a drop of de-ionized water and allowed to dry completely by placing the systems in a vacuum oven at 40 °C for 4 h. SEM images of the above specimen sets were analyzed to confirm the existence of single particles on the substrates so that nanoindentation would not be influenced by their aggregation. The nanoindentation instrument from Triboindenter, Hysitron, Inc., was used with a standard Berkovich diamond three-side pyramid tip of radius 200 nm for indentation tests. On each specimen, nanoindentations were made at least 5 different particles of each substrate and load was 2000 μN.

X-ray photoelectron spectroscopy

X-ray photoelectron spectroscopy (XPS) was used to investigate the surface chemical states of graphite particles. The analysis was performed on an Omnicron ESCA Probe (Omnicron Technology) under 10^{-7} Torr vacuum with an ALKα X-ray source using power of 200 W.

Fourier transform infrared spectroscopy

FT-IR spectroscopy was run on a Perkin-Elmer 1600 FT IR series instrument. Samples were run as pressed KBr pellets. IR absorbance spectra were recorded in the range 400–4,000 cm^{-1} in ambient environment and the resolution was 4 cm^{-1}.

Differential scanning calorimetry test

DSC studies were performed on of the epoxy and GP/epoxy with a TA Instruments DSC Q-10 in standard DSC mode under nitrogen atmosphere at a flow rate of 50 mL/min. In total, 7–10 mg amount of materials of each type was sealed in aluminum hermetic DSC sample pan and equilibrated at 303 K. Dynamic DSC measurements were performed at different heating rates of 10, 15, and 20 K/min over a temperature range from 303 to 593 K. We chose this upper limit because we observed from thermogravimetric analysis (TGA) showing there was a decomposition of epoxy specimens beyond the temperature 593 K and this decomposition would damage the TA instrument. The reaction was considered to be complete when the rate curve leveled off to a base line. The cured samples were then cooled to 303 K temperature rapidly and scanned again at heating rate of 15 K/min to determine the glass transition temperature (T_g). Finally, the specimens were weighed again to compare with initial weight and found that weight losses were negligible in both matrices.

Results and discussion

The XRD patterns of graphite flakes and the ball-milled graphite particles are shown in Fig. 2. The distance

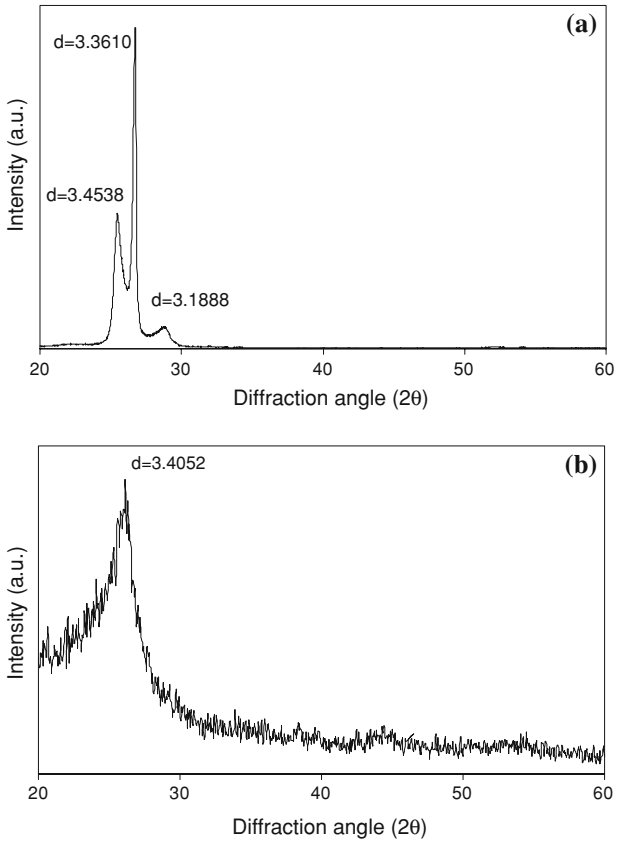

Fig. 2 XRD pattern of the GPs: **a** graphite flakes and **b** GPs

between graphene sheets in the graphite flakes was similar to the original graphite materials, which is 3.37 Å, and this value corresponds to the peak at 26.38° [24]. The GPs had one intense peak at 2θ of 26.15° which corresponds to a d-value of 3.41 Å, and in addition there was a wide range of interlayer distances. Therefore, it is speculated that the GPs were a kind of "puffy" particle with disorders in their graphene layers. TEM image (Fig. 1) confirms this.

From our previous flexural studies, we observed a 20.6% increase of toughness in epoxy composite over pure epoxy (paper submitter to another journal). Though other researchers [25, 26] did not measure toughness, they observed a significant increase of modulus (up to 100%) in different polymer systems with the presence of graphite platelets made by vulcanization of similar expanded graphite flakes. In our case, this increment in modulus was as little as 7.3%. From these observations, it can be speculated that the rigidity of the GPs was reduced, as high rigidity can lead to high modulus and low toughness in the resulting composite material. To confirm this finding accurately, we performed nanoindentation tests on graphite flakes and the GPs; their results are listed in Table 1 which substantiate the above-mentioned conclusions. Taking into consideration both XRD and nanoindentation tests, it can

Table 1 Nanoindentation results

System	Modulus (GPa)	Hardness (GPa)
Graphite flake	73.7127 ± 0.9881	6.0003 ± 0.2075
GPs	41.5761 ± 7.1061	0.7161 ± 0.3102

Note: mean value ± standard deviation

be said that rigidity and hardness of the GPs were reduced in accordance with their loose and "puffed" appearance structure.

Figure 3 shows the XPS spectra of the GPs. This elemental analysis demonstrates the presence of oxygen in the GPs. This oxygen can be part of some functional groups such as –OH, –COOH, –CHO, C–O–C, etc. FT-IR experiment was done to authenticate the presence of these functional groups and its spectrum is shown in Fig. 4. The absorptions in the range of 1720–1050 cm^{-1} and 665 cm^{-1} represent the presence of –COOH, –OH, C–O–C and C=O functional groups. The presence of carboxyl functional groups can also be detected at around 1,650 cm^{-1}. Other researchers also observed similar functional groups [27–31]. Both these XPS and FT-IR results indicated that due to acid treatment and heating at high temperature on the graphite materials assisted in oxidization of some carbon double bonds, leading to the presence of oxygen-containing functional groups in the graphite particles.

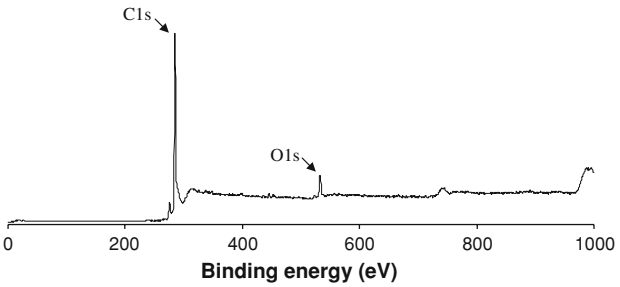

Fig. 3 XPS spectrum of the GPs

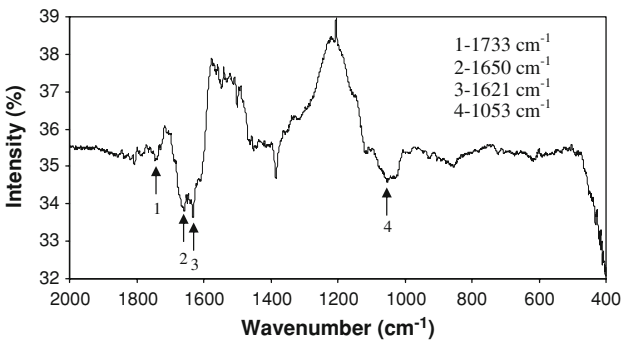

Fig. 4 FT-IR spectrum of the GPs

Table 2 Peak temperatures and heat of reaction

Specimen	10 K/min		15 K/min		20 K/min	
	T_p	ΔH	T_p	ΔH	T_p	ΔH
Epoxy	473	255.3	488	223.8	496	206.5
GP/epoxy	474	204.8	492	187.2	496	155.6

Note: T_p in K and ΔH in J/g

Table 2 lists the exothermic peak temperatures, T_p, and heats of reaction ΔH for both pure epoxy and GP/epoxy system. From this table, it can be observed that incorporation of the GPs into the epoxy markedly affected the curing reaction of the epoxy. For each heating rate, heat of curing reaction, ΔH, for the GP/epoxy, was smaller than that of the pure epoxy. As a certain amount of the GPs was present in the GP/epoxy system, the amount of the epoxy in the GP/epoxy system was less than the amount of epoxy in the pure epoxy system. This decrease in epoxy concentration may be the reason for the reduction in the heat of curing for the GP/epoxy system, especially when there was the requirement of at least two monomer points to react to each other as discussed earlier. However, there were no significant changes in T_p due to the addition of GPs in the epoxy. When curing proceeds, epoxy monomer molecules react with each other and a network forms. For a reaction to occur, a certain amount of thrust is needed and for this, reactant molecules should be in optimal proximity. If the distance between reactants is more than optima level, more energy will be needed to compensate the thrust force, and this can be done at higher temperature. However, a media in-between reactant molecules which can provide more thrust may balance the energy needed for a reaction to take place. Graphite materials have higher thermal conductivity, and at the same temperature they have atomic motions of higher amplitude than epoxy. This higher molecular motion balances the thrust required for the epoxy molecules separated by the graphite particles. Therefore, peak temperature T_p in the GP/epoxy system was more or less equal to that in the pure epoxy system. Further, the presence of carboxyl groups as well as other strong hydrogen bonding acids and alcohols in the graphite particles may be responsible for the enhancement of curing rate through the impurity catalysis mechanism [32]. Comparing the data, it can be stated that in this study, although the GPs had a retarding effect on curing reaction of the epoxy, the effect was trivial, i.e. not as much as observed by other researchers [13–17].

In addition, it can be found that with the change of heating rate for a particular epoxy system, there were both a decrease in ΔH and an increase in T_p (Table 2). The curing of pure epoxy with amine-type curing agent involves several different reactions as described earlier. The rates of these reactions vary with the temperature in different ways. Change of heating rate may favor one reaction with respect to another, and thus affects the total curing reaction and molecular structure of the crosslinked network. Moreover, with higher heating rate, there is a possibility of the existence of temperature gradient over the epoxy material and the reaction between epoxy molecules would vary from place to place within the system. At the same time, with higher heating rate, an epoxy molecule does not pose similar reactivity for a long time and therefore reactivity of epoxy molecules also varies from place to place. In fact, quick changes of reactivity and other parameters are not favorable for better curing reaction, and they inhibit the curing reactions. Less curing reaction means less amount of heat of reaction, and curing will take place only at higher temperature due to an unfavorable environment. For these reasons, peak temperatures are higher at higher heating rate.

In Fig. 5a, α versus T graphs for the pure epoxy and the GP/epoxy system at heating rate of 10 K/min are given. A sigmoid-shaped curve for each specimen, which indicates the autocatalytic reaction [33], also occurred in the GP/epoxy system, i.e. addition of the GPs did not change the curing reaction mechanism. It is seen that at the beginning, the extent of fractional conversion in the GP/epoxy material was in advance compared to that in pure epoxy and, as the temperature increased, one mingled with other. Therefore, at a low heating rate, addition of the GPs *enhanced* the degree of curing instead of delaying as observed by others [13–17]. This effect is a positive role in composite processing as the GP/epoxy mixture would need less or no post-cure time than the pure epoxy processing. The possible mechanism behind this phenomenon can be explained by molecular motions and interactions. For the occurrence of a certain reaction, the reactant molecules need a certain amount of thrust as mentioned before. Inclusion of the GPs introduced two events in the epoxy resin: (1) increase in viscosity and (2) increase in separation of epoxy molecules and therefore recession of curing reaction was expected. On the other hand, the GPs used in this study with low rigidity and higher specific surface area are members of the carbon material family that has a *higher thermal conductivity* compared to any pure epoxy resin. It can be speculated that the molecular motion in the GP/epoxy mixture was not to be delayed due to the addition of the GPs. A good dispersion of the GPs in the GP/epoxy mixture could help transfer heat throughout the GP/epoxy mixture while curing, thus compensating the less curing in epoxy due to presence of the GPs. In addition, presence of carboxyl groups as well as other strong hydrogen bonding acids and alcohols in the graphite particles may be responsible for enhancement of curing degree [32]. However, at high heating rate, the GPs did not show

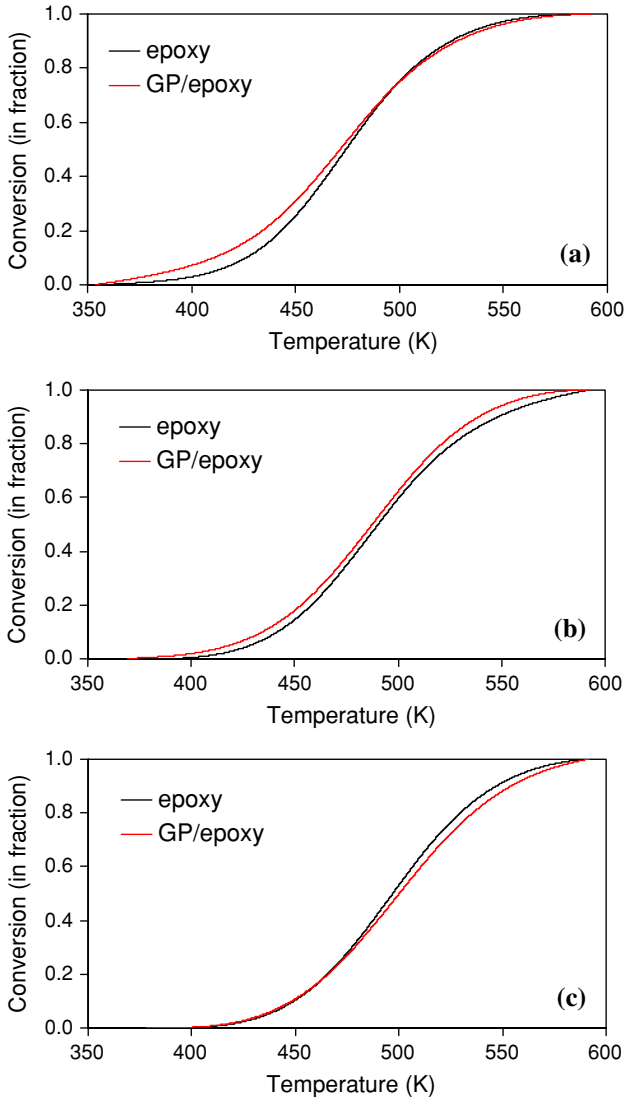

Fig. 5 α as a function of temperature for non-isothermal cure of pure epoxy and GP/epoxy under different heating rates: **a** 10 K/min, **b** 15 K/min and **c** 20 K/min

any advantage in curing and high-temperature gradient, discrete zone curing, and uneven curing with unfavorable environment as explained earlier might be the possible reasons behind this phenomenon.

Almost a similar trend can be observed in Fig. 5b and c, which illustrate curing conversions of the pure epoxy and the GP/epoxy mixture at heating rates of 15 and 20 K/min, respectively. At 15 K/min heating rate, the GP/epoxy mixture was well advanced throughout the curing process. However, at 20 K/min, pure epoxy has higher curing conversion compared to the GP/epoxy mixture in later stage. The reasons may be that high heating rate provided less time for the spreading of heat to the far point and hindered molecular motion of the GPs due to gradual solidification of the epoxy resin with time.

In the vitrification phase of the curing process, the curing is a diffusion controlled process and reaction rates $d\alpha/dt$ and $d\alpha/dT$ decrease. To find out the effect of the GPs on degree of vitrification of the pure epoxy, the α versus T curves at different heating rates can be superimposed on a master reference (if all the curves have same functional form) to compare with each other [15] by shifting along a temperature axis and then a shift factor could be developed to characterize the vitrification phenomena (this is a kind of qualitative analysis). The shift factor, $\phi(\beta) = T_{\text{ref}} - T_{\beta}$, where β is the heating rate and T_{ref} is the temperature in reference curve, can be considered an arbitrary reference among the three heating rates. In this study, the curve at a heating rate of 20 K/min has been considered as master curve and therefore $\phi(\beta) = T_{\text{ref}} - T_{\beta}$ will always be positive which will assist to find the tendency of other parameters discussed later.

The reaction rate, $d\alpha/dt$, expression can be obtained [10–12]:

$$\frac{d\alpha}{dt} = A\exp(E_c/RT)f(\alpha) \tag{1}$$

Suppose $T = \beta t$, where β is the heating rate and t is the time and Eq. 1 can be termed as:

$$\frac{d\alpha}{dT} = A\exp(E_c/RT)\frac{f(\alpha)}{\beta} \tag{2}$$

Taking logarithm,

$$\ln\left(\frac{d\alpha}{dT}\right) - \ln[Af(\alpha)] = -\frac{E_c}{RT} - \ln\,\beta \tag{3}$$

The values of $\ln[Af(\alpha)]$ in the curves at different heating rates are equal as far as arbitrary α is concerned [15]. However, the values of $d\alpha/dT_{\beta}$ and $d\alpha/dT_{\text{ref}}$, the tangent slopes of a point corresponding to conversion α at a particular heating rate β and at a reference heating rate (master), respectively, are not always equal. If $d\alpha/dT_{\beta} = d\alpha/dT_{\text{ref}}$, from Eq. 3 there can be an expression as:

$$\ln[Af(\alpha)] - \frac{E_c}{RT_{\beta}} - \ln\,\beta = \ln[Af(\alpha)] - \frac{E_c}{RT_{\text{ref}}} - \ln\,\beta_{\text{ref}}$$

$$-\frac{E}{RT_{\beta}} - \ln\,\beta = -\frac{E}{RT_{\text{ref}}} - \ln\,\beta_{\text{ref}}$$

$$\frac{1}{T_{\beta}} - \frac{1}{T_{\text{ref}}} = R\left(\frac{\ln(\beta_{\text{ref}}/\beta)}{E}\right)$$

$$T_{\text{ref}} - T_{\beta} = T_{\beta}T_{\text{ref}}R\left(\frac{\ln(\beta_{\text{ref}}/\beta)}{E}\right) \tag{4}$$

As the reference curve was curing curve at heating rate of 20 K/min,

$$T_{\text{ref}} - T_{\beta} > 0$$

$$\beta_{\text{ref}}/\beta > 1$$

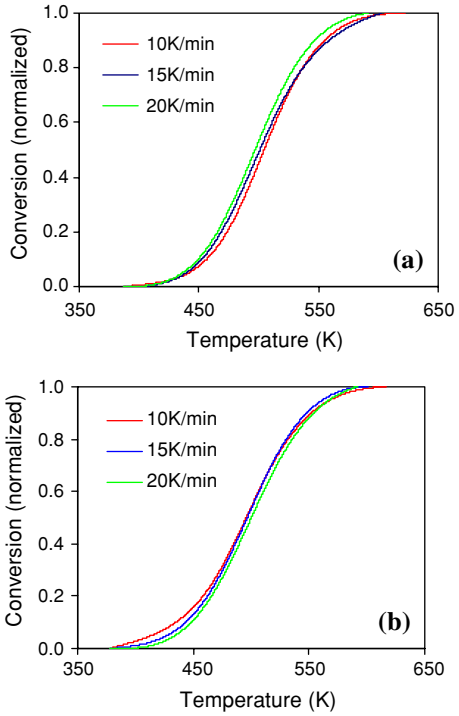

Fig. 6 Superimposed curves of α as a function of temperature for non-isothermal cure: **a** pure epoxy and **b** GP/epoxy

Observing the trend (image not included), it can be said that $T_{\text{ref}}T_{\beta}$ will increase consistently with the increase of α (except near to the full conversion). Therefore, $T_{\text{ref}} - T_{\beta}$ will show consistent increment, increasing with α (considering Eq. 4), i.e. $\mathrm{d}\alpha/\mathrm{d}T_{\beta} > \mathrm{d}\alpha/\mathrm{d}T_{\text{ref}}$. When T_g crosses the curing temperature, a thermoset resin vitrifies and the degree of vitrification phenomena increases if the value of $\mathrm{d}\alpha/\mathrm{d}T_{\beta} - \mathrm{d}\alpha/\mathrm{d}T_{\text{ref}}$ decreases, i.e. the reference curve and comparative curve are nearer to each other [15]. Therefore, observing Fig. 6a and b which show the superimposed curves on a master curve, it can be speculated that GPs minutely instigated the vitrification phenomena in the pure epoxy. This inference may be confirmed by comparing T_gs of the pure epoxy and the GP/epoxy system listed in Table 3. There was an increment in T_g of pure epoxy with the inclusion of the GPs. Generally with inclusion, T_g goes down [15], therefore a small increment is a positive indication in curing of epoxy with the GPs. On the molecular scale, T_g represents the mobility level of polymer chain/network in the material. An increase in T_g corresponds to a decrease in mobility in the polymer segments of the chains [34]. Moreover, the GPs did not inhibit the cure reaction severely as mentioned before, resulting in almost no change or minor change in crosslinking density in epoxy resin with the GPs and therefore no lower T_g. Thus, T_g increased over curing temperature in the GP/epoxy and therefore the GPs could facilitate the occurrence of vitrification phenomena in epoxy though this effect may be small.

Table 3 Glass transition temperature and activation energy (in constant energy method)

System	T_g (K)	E_c (kJ mol^{-1})	Correlation coefficient (regression analysis)
Epoxy	416	44.83	0.9997
GP/epoxy	418	48.05	0.9902

The impact of the GPs on kinetic parameters of curing reaction of the epoxy was also studied. The assumption that the heat evolved in the curing reaction is proportional to the extent of reaction represents the notion that at the peak exotherm at any heating rate, the fractional extent of conversion α is constant for a particular system [35, 36]. It is observed (image not included) that α is constant (∼0.5) at the peak exotherm at different heating rates for both epoxy and GP/epoxy. Therefore, Ozawa equation [36] as written next can be used to calculate the activation energy for each system.

$$\frac{\mathrm{d}(-\ln\beta)}{\mathrm{d}(1/T_p)} = \frac{1.502E_c}{R} \tag{5}$$

Using linear regression analysis in –ln β versus $1000/T_p$ plots (using Eq. 5) of the pure epoxy and the GP/epoxy mixture, their activation energies (E_c) were calculated as listed in Table 3. It shows that incorporation of GPs slightly increased the activation energy in pure epoxy.

The possible reasons were enhancement of both the viscosity of pure epoxy systems and separation of epoxy molecules for incorporation of the GPs. The increase in activation energy implies that GPs inhibited the curing process. However, from Fig 5, it can be observed that curing conversion of pure epoxy with respect to temperature was not restrained by the GPs. It is believed that at higher temperature, higher molecular motion of the GP molecules than to epoxy molecules countered the hindrance of the curing process.

As discussed earlier, for the thermosetting resins which follow autocatalytic kinetics (excluding diffusion controlled, fusion and inversion type reactions), $f(\alpha)$ (Eq. 1) has a generalized expression as shown next:

$$f(\alpha) = (1-\alpha)^n\alpha^m \tag{6}$$

where $m + n$ is the overall order of reaction [37, 38]. Then we have:

$$\ln\left(\frac{\mathrm{d}\alpha}{\mathrm{d}t}\right) = \ln A - \frac{E_c}{RT} + n\ln(1-\alpha) + m\ln\alpha \tag{7}$$

From Eq. 7:

$$\ln\left(\frac{\mathrm{d}(1-\alpha)}{\mathrm{d}t}\right) = \ln A - \frac{E_c}{RT'} + n\ln\alpha + m\ln(1-\alpha) \tag{8}$$

Combining Eqs. 7 and 8:

$$\text{Value I} = [(E_c/RT) + \ln(d\alpha/dt)] - [E_c/RT' + \ln(d(1-\alpha)/dt)] = 2\ln A + (n+m)\ln[\alpha(1-\alpha)] \quad (9)$$

Then, Eq. 7 − Eq. 8 gives:

$$\text{Value II} = [(E_c/RT) + \ln(d\alpha/dt)] - [E_c/RT' + \ln(d(1-\alpha)/dt)] = (n-m)\ln[(1-\alpha)/\alpha] \quad (10)$$

DSC curves for the epoxy and the GP/epoxy systems at heating rate of 15 K/min were studied to find the curing parameters. The values of $n + m$ and 2 ln A were obtained from the slope and intercept of the plot of Value I versus ln[$\alpha(1 - \alpha)$] (using Eq. 9) for the pure epoxy and the GPs/epoxy. The values of $n - m$ were obtained from the slope of the plot of Value II versus ln[$(1 - \alpha)/\alpha$] (using Eq. 10) for the pure epoxy and the GP/epoxy composite. The values of these different parameters and the curing kinetic equations are tabulated in Tables 4 and 5, respectively. From these tables, it can be contemplated that the incorporation of the GPs increased the values of parameters of the pure epoxy; however, the increment was not substantial enough compared to the values of similar parameters observed in others studies [15–17]. This indicates that despite some sub-step improvements, overall the GPs did not influence the curing process of pure epoxy appreciably.

In the above-mentioned study, the calculated E_c (using constant activation energy method) can be considered as apparent activation energy of the global reaction. In fact, the reaction of curing of epoxy is very complex, and it is possible that the activation energy would change in every possible fraction of time. In this study, an effort was made to calculate the variable activation energy, E_α, as a function of extent of conversion without any assumption about the reaction mode. The following equation can be stated from Eq. 1

$$\ln(d\alpha/dt) = \ln[Af(\alpha)] - (E_\alpha/RT) \quad (11)$$

It is expected that the plot of ln($d\alpha/dt$) versus ($1/T$) (using Eq. 11) would be a straight line with slope E_α/R and an intercept of ln[$Af(\alpha)$]. The data points for each straight line were obtained from DSC curves at different heating rates considering same fractional extent of conversion (α). By repeating the procedure, the values of E_α and ln[$Af(\alpha)$] corresponding to different α were acquired.

Table 5 Equations of curing kinetics (in constant method)

System	Curing kinetic equation
Epoxy	$d\alpha/dt = e^{11.5}e^{(-44.83/RT)}(1-\alpha)^{1.158}\alpha^{0.09}, \quad \alpha \in [0,1]$
Epoxy/GNP	$d\alpha/dt = e^{10.0}e^{(-48.05/RT)}(1-\alpha)^{1.233}\alpha^{0.21}, \quad \alpha \in [0,1]$

Figures 7a and b shows the plots of ln($d\alpha/dt$) versus ($1/T$) for the pure epoxy and the GP/epoxy, respectively. A set of α was considered from the full range of experimental data, i.e. α = 0.05, 0.10, 0.15……, 0.90 and 0.95. Using linear regression method on each set of data linked to a particular α, the values of E_α and ln[$Af(\alpha)$] were obtained. Figure 8a and b shows the plot of E_α versus α for the pure epoxy and the GP/epoxy, respectively. From the figures, it can be observed that the values of E_α were different for different values of α though the variation of E_α was not broad in pure epoxy. Therefore, it can be said that inclusion of GPs produced a variation of E_α in the epoxy systems.

Polynomial regression methods were used to fit a curve to the data, and it was observed that a cubic polynomial could be sufficient to fit as shown in Fig. 8a and b for both systems. The fitted equation for GP/epoxy system is given as:

$$E_\alpha(\alpha) = 30.218 + 149.04\alpha - 377.07\alpha^2 + 300.2\alpha^3, \quad \alpha \in (0,1)$$

Differentiating $E_\alpha(\alpha)$ with respect to α,

$$dE_\alpha/d\alpha = 149.04 - 754.08\alpha + 900.6\alpha^2$$

$$dE_\alpha/d\alpha = 0 \quad (\alpha \approx 0.32,\ 0.52)$$

Therefore, there are two value of $E_\alpha(\alpha)$, where $dE_\alpha/d\alpha = 0$; one is E_α = 49.13 kJ/mol and another is E_α = 47.97 kJ/mol. At the beginning, the value of E_α was 34.94 kJ/mol ($\alpha = 0.05$) and then increased to 49.13 kJ/mol ($\alpha \approx 0.32$). Next to it, the value of E_α decreased to 47.97 ($\alpha \approx 0.52$), and thereafter increased to 92.65 kJ/mol. For both systems, concerned values and equations are listed in Table 6.

From the above-mentioned analyses, it seems that the variable E method is more effective in studying the cure kinetics of the polymer compared to constant E method. Constant E method depends on only peak temperatures of the curing DSC curves, whereas variable E method utilizes most of the values of the curves. In calculation $d\alpha/dt$ versus α curve, constant E method uses one heating rate at a time, while variable E method uses all three heating rates.

Table 4 Curing parameters at heating rate of 15 K/min

System	$n + m$	2 ln A	Correlation coefficient	$n - m$	Correlation coefficient	n	m	A
Epoxy	1.2532	23.014	0.99914	1.0631	0.99513	1.158	0.095	$e^{11.5}$
GP/epoxy	1.4445	20.041	0.99934	1.0217	0.99784	1.233	0.211	$e^{10.0}$

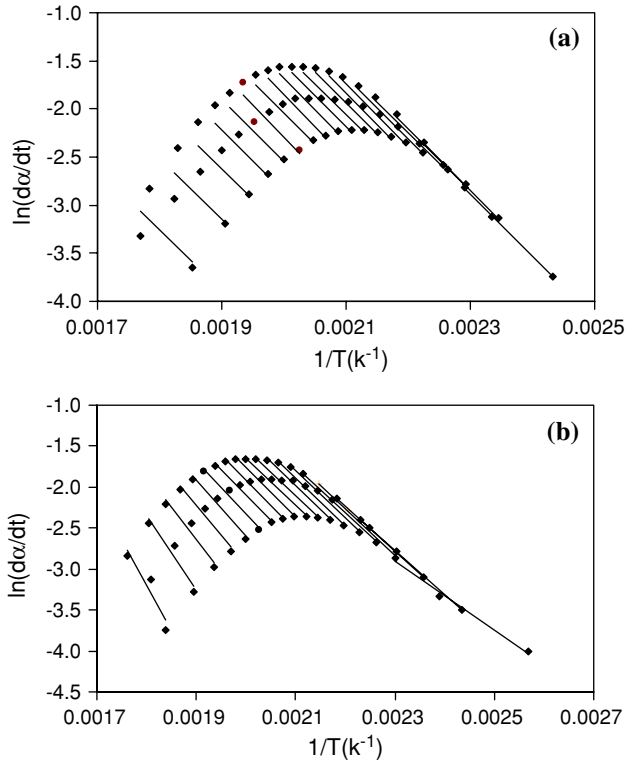

Fig. 7 $\ln(\mathrm{d}\alpha/\mathrm{d}t)$ versus $1/T$ plots: **a** pure epoxy and **b** GP/epoxy

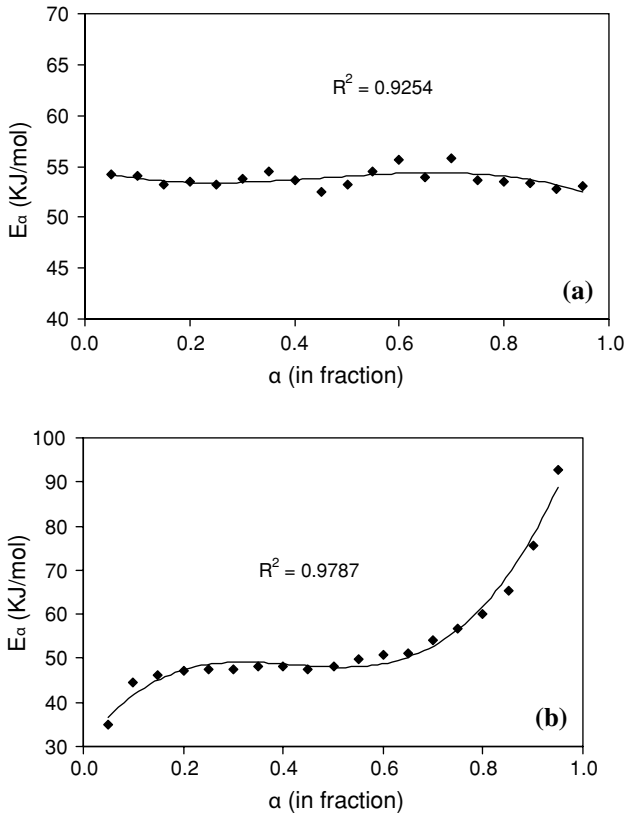

Fig. 8 Dependence of activation energy (E_α) on the fractional extent of conversion (α): **a** pure epoxy and **b** GP/epoxy

Table 6 Activation energies E_α (in variable energy method)

Pure epoxy	
E_α, $\alpha \in (0,1)$	$54.754 - 12.808\alpha + 35.781\alpha^2 - 26.127\alpha^3$
Variation of $\mathrm{d}E_\alpha/\mathrm{d}t$	$0 < \alpha \leq 0.24$, $\mathrm{d}E/\mathrm{d}\alpha \leq 0$; $0.24 < \alpha \leq 0.66$, $\mathrm{d}E/\mathrm{d}\alpha > 0$, $0.66 < \alpha < 1$, $\mathrm{d}E/\mathrm{d}\alpha \leq 0$
Scope of E_α (kJ/mol)	52.47–55.78
GP/epoxy	
E_α, $\alpha \in (0,1)$	$30.218 + 149.04\alpha - 377.07\alpha^2 + 300.2\alpha^3$
Variation of $\mathrm{d}E_\alpha/\mathrm{d}t$	$0 < \alpha \leq 0.32$, $\mathrm{d}E/\mathrm{d}\alpha \geq 0$; $0.32 < \alpha \leq 0.52$, $\mathrm{d}E/\mathrm{d}\alpha < 0$, $0.52 < \alpha < 1$, $\mathrm{d}E/\mathrm{d}\alpha > 0$
Scope of E_α (kJ/mol)	34.94–92.65

Moreover, E_α has been evaluated without any assumption regarding any reaction model starting from the basic equation. Therefore, evaluation of the curing kinetics using variable activation energy is more pragmatic.

From Fig. 8, it can be observed that in the pure epoxy, requirement of activation energy did not vary much (52.47–55.78 kJ/mol) throughout the curing process, whereas in the GP/epoxy, it varied from 34.94 to 92.65 kJ/mol. Pure epoxy is a homogeneous material and therefore some phenomena such as etherification, motion of chain segments, free volume, etc., were responsible for changes in activation energy. At the early stages of the curing process, the most influential participants were monomers or very small chain segments with loose packing which provided sufficient space to segments to move around. This cooperative motion of the segments caused the decrease in activation energy (Fig. 8a). At later stages, the activation energy increased. As the cure reaction proceeded, the fraction of conversion, α, increased and free volume decreased. In the glassy state, a small amount of free volume was available for local motion of chain segments, and thus a great degree of cooperation between chain segments was needed to achieve a segmental motion as explained earlier. An energy barrier between segments occurs due to this cooperative behavior, and therefore a higher activation energy, was needed in the later stage. The enhancement of activation energy was comparatively low, and especially at the very end stage, the activation energy decreased, possibly due to less reaction occurring.

From the results of activation energy required for the GP/epoxy (Fig. 8b), a trend of change of activation energy with extent of fraction of conversion can be established, and it is shown to have three characteristic stages of activation energy with respect to extent of conversion fraction. The first stage was characterized by a sharp increase of the activation energy. The second stage, which extended from $\alpha = 0.20$ to $\alpha = 0.80$, indicated that the values of the activation energy were almost constant and the third stage was again characterized by a higher increase of activation

energy. The second stage is similar to pure epoxy system in terms of amount of activation energy.

In the GP/epoxy, at the beginning of conversion (before gelation), a lesser amount of activation energy compared to that in the pure epoxy was required. Effects of higher mobility of graphite atoms and low concentration of epoxy resin may be the reasons for this phenomenon. Another reason may be the presence of different chemical groups in GPs, which brought some epoxy molecules to the threshold of some chemical reactions, and a slight amount of heat energy was sufficient for those chemical reactions to occur. With the increase in conversion fraction, an increase in activation energy was observed (Fig. 8b). The graphite particles were comparatively heavier than epoxy resin molecules, therefore these particles could be seen as obstacles to free movement of molecules. In addition, with more conversion of the pure epoxy the viscosity of the GP/epoxy system increased and movement of epoxy molecules decreased. To initiate a translational motion of epoxy molecules, a great degree of cooperation between molecules was needed. This cooperation between epoxy molecules generated an additional amount of energy barrier to the motion of molecules and a higher amount of activation energy was needed for the conversion.

As more conversion occurred, both the crosslinking degree and number of segments increased, and at this point the stoichiometric effect of the graphite particles on curing conversion was comparatively equal to that of epoxy crosslinked segments. Therefore, at this stage (second stage), extra energy was not needed for the conversion until the amount of conversion was such that a comparatively higher hindrance came into play. In the GP/epoxy, there was an enhancement in activation energy at the later stage (third stage) (Fig. 8b). At higher conversion stage, formation of epoxy network around the GPs was greater compared to that in other regions. Stoichiometric effects of the GPs surrounded by the larger epoxy network and glassy transition of the epoxy with the increase of viscosity were responsible for the hindrance to curing. In addition, at this stage, diffusion control had a profound effect on curing kinetics and the curing rate was lower. In diffusion controlled zone, most of the vitrification takes place and this causes the higher value of activation energy at the final cure stage.

Conclusions

Effects of GPs (1 wt%) composed of disordered and puffed graphene sheets on the curing kinetics of an epoxy (diglycidyl ether of bisphenol-A based) were studied. Curing reactions with three different heating rates were analyzed. The curing kinetic parameters of the pure epoxy and the GP/epoxy were obtained by constant energy and variable energy methods. Curing conversion versus temperature curves in each epoxy system showed the sigmoidal shape, which indicated that the GPs did not change the curing mechanism, i.e. autocatalytic kinetics also occurred in the GP/epoxy system. There were enhancements in activation energy E_c, glass transition temperature T_g and reduction in total heat of reaction ΔH due to incorporation of the GPs in the epoxy. However, the effect of the GPs on peak temperatures T_p at different heating rates showed no correlation. Results on the GP/epoxy system from the variable activation energy method revealed that at the beginning of curing, the activation energy was low and increased to a constant stage followed by an increased stage to the end of curing reaction, while in the pure epoxy, the variation of activation energy with curing conversion was very limited. It was also observed that inclusion of the GPs increased the degree of vitrification of the epoxy slightly. Considering all the parameters observed in this study, it can be concluded that the thermally conductive GPs in epoxy did not significantly impede or enhance the curing process. Reduced rigidity of the GPs with their carboxyl groups and their higher thermal conductivity compensated for the hindrance of the curing reaction in the epoxy. Therefore, the GPs reinforced the epoxy system (as observed in our other reported studies) without appreciably inhibiting the curing reaction of the epoxy resin. It can also be considered that the GP/epoxy composite with lower amount of the GPs can be processed with the curing parameters used for the neat epoxy.

The information obtained from this study provides a greater understanding of the multiple factors involved in the relationship between structure and properties of the composites, which can lead to enabling improvement of the composite functionalities without creating processing penalties.

Acknowledgement This work was supported from NSF through NIRT grant 0506531 and GOALI 0758251.

References

1. Donnet JB (2003) Compos Sci Technol 63:1085
2. Frisch HL, Mark JE (1996) Chem Mater 8:1735
3. Brown EN, While SR, Sottos NR (2004) J Mater Sci 39:1703. doi:10.1023/B:JMSC.0000016173.73733.dc
4. Jang BZ (1994) Advanced polymer composites: principles and applications. ASM International, Materials Park, OH
5. Chand S (2000) J Mater Sci 35:1303. doi:10.1023/A:1004780301489
6. Krumova M, Klingshirn C, Haupert F, Friedrich K (2001) Compos Sci Technol 61:557
7. Wong SC, Sutherland EM, Uhl FM (2006) Mater Manuf Processes 20:159
8. Tronc F, Chen W, Winnik MA, Eckersley ST, Rose GD, Weishuhn JM, Meunier DM (2002) J Polym Sci A Polym Chem 40:4098

9. Liu H, Uhlherr A, Bannister MK (2004) Polymer 45:2051
10. Prime RB (1981) In: Turi EA (ed) Thermal characterization of polymeric materials, chap 5. Academic Press, New York
11. Apicella A, Nicolais L, Iannone M, Passerini P (1984) J Appl Polym Sci 29:2083
12. Barton JM (1985) In: Dusek K (ed) Epoxy resins and composites. Advances in polymer science, vol 72. Springer-Verlag, Berlin, p 110
13. Buggy M, Temimhan T, Braddell O (1996) J Mater Process Technol 56:292
14. Zhong WH, Li J, Lukehart CM, Xu LR (2005) Polym Compos 26:128
15. Zhou T, Gu M, Jin Y, Wang J (2005) Polymer 46:6216
16. Pluart LL, Duchet J, Sautereau H (2005) Polymer 46:12267
17. Ton-That MT, Ngo TD, Ding P, Fang G, Cole KC, Hoa SV (2004) Polym Eng Sci 44:1132
18. Chan CM, Wu J, Li JX, Cheung YK (2002) Polymer 43:2981
19. Wang Q, Storm BK, Houmoller LP (2003) J Appl Polym Sci 87:2295
20. Kaelble DH, Dynes PJ, Cirlin EH (1974) J Adhesion 6:23
21. Grenier-Loustalot MF, Grener P (1992) Polymer 33:1187
22. Phelan JC, Sung CSP (1997) Macromolecules 30:6845
23. Rokhlin SI, Segal E (1985) J Mater Sci 20:3300. doi:10.1007/BF00545198
24. Yasmin A, Daniel IM (2004) Polymer 45:8211
25. Cho J, Chen JY, Daniel IM (2007) Scr Mater 56:685
26. Mack JJ, Viculis LM, Ali A, Luoh R, Yang G, Hahn HT, Ko FK, Kaner RB (2005) Adv Mater 17:77
27. Lerf A, He H, Foster M, Klinowski J (1998) J Phys Chem B 102:4477
28. Sutherland EM (2005) A master thesis, North Dakota State University
29. Cassagneau T, Fendler JH (1998) Adv Mater 10:878
30. Scholz W, Boehm HP (1969) Z Anorg Allg Chem 369:327
31. Ramesh P, Sampath S (2001) Analyst 126:1872
32. Wise CW, Cook WD, Goodwin AA (2000) Polymer 41:4625
33. Levenspiel O (1972) Chemical reaction engineering, 2nd edn. Wiley, New York, p 56
34. Wiederhorn SM (1984) Annu Rev Mater Sci 14:373
35. Donnellan T, Roylance D (1982) Polym Eng Sci 13:821
36. Ozawa T (1965) Bull Chem Soc Jpn 38:1881
37. Wendlandt WW (1986) Thermal analysis. Wiley, New York, p 269
38. Kamal MR, Sourour S (1973) Polym Eng Sci 13:59